ELSEVIER

Journal of Immunological Methods 285 (2004) 145–155

JIM
Journal of
Immunological Methods

www.elsevier.com/locate/jim

Quantification of vascular endothelial growth factor-C (VEGF-C) by a novel ELISA

Herbert A. Weich[a,*], Hiroko Bando[a], Maren Brokelmann[a], Petra Baumann[b], Masakazu Toi[c], Bernhard Barleon[d], Kari Alitalo[e], Bence Sipos[f], Jonathan Sleeman[b]

[a] *Department of Gene Regulation and Differentiation National Research Centre for Biotechnology (GBF), Mascheroder Weg 1, 38124 Braunschweig, Germany*
[b] *Forschungszentrum Karlsruhe, Institute of Toxicology and Genetics, 76021 Karlsruhe, Germany*
[c] *Tokyo Metropolitan Komagome Hospital, Japan*
[d] *RELIATech GmbH, 38124 Braunschweig, Germany*
[e] *Cancer Biology Laboratory, University of Helsinki, Finland*
[f] *Department Pathology, University of Schleswig-Holstein, Campus Kiel, Germany*

Received 7 August 2003; received in revised form 30 September 2003; accepted 30 October 2003

Abstract

Lymphangiogenesis plays an important role in several normal and pathological conditions such as wound healing, inflammation or metastasis formation in several malignancies. VEGF-C and VEGF-D are important and specific regulatory factors for lymphatic endothelial proliferation and lymphangiogenesis. In order to develop a highly sensitive and specific detection system for VEGF-C, we produced soluble binding proteins and antibodies for a microtiterplate-based assay. Here we describe a specific enzyme-linked immunosorbent assay (ELISA) for the measurement of human, rat and murine VEGF-C. The different antibodies developed against human and rat VEGF-C could be combined to detect processed and partially processed VEGF-C in a specific way. The ELISA was able to detect human and rat VEGF-C with a minimum detection limit of 100 pg/ml. The assay did not show any cross-reactivity with the related protein VEGF-D. Furthermore, complex formation with its soluble receptors VEGFR-2 and VEGFR-3 did not restricted the sensitivity of the assay. Using this assay, VEGF-C was measured in supernatants and lysates of different cell types and in tumour tissue samples of murine, rat and human origin. Cell lines secrete VEGF-C in very low amounts (<1 ng/ml) whereas VEGF-C transfected cells can secrete up to 50 ng/ml VEGF-C into the supernatant. In human tumour tissue samples VEGF-C was detected in some carcinomas in the low protein range. This ELISA will be a useful tool for investigations concerning the physiological function of VEGF-C in lymphangiogenesis under normal and pathophysiological conditions.

Keywords: VEGF-C; Sandwich-ELISA; Lymphangiogenesis; Growth factors

Abbreviations: VEGF, vascular endothelial growth factor; VEGFR-1, vascular endothelial growth factor receptor 1; KDR, kinase domain region receptor; flt-1, *fms*-like tyrosine kinase; VEGFR-3, vascular endothelial growth factor receptor 3; ELISA, enzyme-linked immunosorbent assay.

* Corresponding author. Department RDIF, GBF, Mascheroder Weg 1, D-38124 Braunschweig, Germany. Tel.: +49-531-6181-445; fax: +49-531-6181-202.
E-mail address: weich@gbf.de (H.A. Weich).

0022-1759/$ - see front matter © 2004 Elsevier B.V. All rights reserved.
doi:10.1016/j.jim.2003.10.015

1. Introduction

The growth of lymphatic vessels is called lymphangiogenesis and occurs after tissue injury, obstruction or damage of lymphatic vessels (Junghans and Collin, 1989). The lymphatic system serves to reduce the increased tissue pressure associated with edema and inflammation (Pullinger and Florey, 1937). In the last 5–7 years a picture has emerged, that the receptor tyrosine kinase VEGFR-3 (Flt-4) and its ligands are the key players in the molecular regulation of lymphangiogenesis (Korpelaionen and Alitalo, 1998). The two ligands VEGF-C and VEGF-D induce the phosphorylation of VEGFR-3 and regulate the growth and differentiation of lymphatic endothelium (LE) either alone or in combination with other growth factors (Joukov et al., 1996; Achen et al., 1998). Both ligands are members of the PDGF/VEGF super family and are virtually identical in their molecular properties. They are produced as precursor molecules and then progressively processed during their biosynthesis to remove the N- and C-terminal ends of the proteins (Joukov et al., 1997a,b). This processing increases the affinity of VEGF-C and VEGF-D for VEGFR-3 (Joukov et al., 1997a; Achen et al., 1998), but fully processed forms of both ligands have been demonstrated to activate also VEGFR-2. Although they are less potent activators of VEGFR-2 than of VEGFR-3, they contribute to normal angiogenesis (Achen et al., 1998; Joukov et al., 1997a,b; Stacker et al., 1999). However, after binding to VEGF-C and VEGF-D, VEGFR-3 is capable of transducing signals triggering the proliferation of VEGFR-3 expressing cells in vitro and in vivo (Jeltsch et al., 1997; Oh et al., 1997; Veikkola et al., 2001). Blocking of VEGFR-3 activation inhibits the formation of lymphatic vessels in the developing embryo (Oh et al., 1997). VEGFR-3 and its ligands may play an important role in several pathologic conditions where lymphangiogenesis occurs or the function of the lymphatics is involved. More recent studies suggest that patients with mutations in the VEGFR-3 gene develop lymphedema (Irrthum et al., 2000; Karkkainen et al., 2000). However, several normal tissues (e.g. heart and lung) are also known to express high rates of VEGF-C gene. This suggests that VEGF-C is probably necessary for tissue homeostasis but the exact physiological role is unknown (Joukov et al., 1997a,b; Kirkin et al., 2001). Very recently, an indirect ELISA was established for the measurement VEGF-C in plasma samples from cancer patients (Duff et al., 2003). In this assay, it was not possible to use purified VEGF-C standards, and for that reason only indirect statements can be made about the amount and distribution of VEGF-C in plasma samples. According to this report, colorectal cancer patients have three-fold increased VEGF-C levels in plasma compared to controls (Duff et al., 2003).

For the detection of VEGF-C protein production and secretion in human tissue and in animal models, a reliable and sensitive assay has hitherto not been available so. The objective of this work was therefore to develop such an assay for the detection and quantification of processed forms of VEGF-C. This goal was achieved by establishing of a sandwich ELISA format for VEGF-C that can be used to detect and measure VEGF-C in human tissue, tumours and in several animal or cellular models. VEGF-C amounts in the picogram range can be measured with this new ELISA, and we present here quantitative data for VEGF-C in human tissue samples and various cell culture supernatants for the first time.

2. Materials and methods

2.1. Proteins and antibodies

The fully processed rat protein dNdC-VEGF-C and dNdC-VEGF-D were produced in insect cells and purified from supernatants as previously reported (Kirkin et al., 2001). The processed rat VEGF-C is virtually identical to mouse VEGF-C. Human dNdC-VEGF-C and soluble VEGFR-3 production was achieved as described before (Joukov et al., 1997a,b; Hornig et al., 1999). Because all commercially available antibodies against VEGF-C were found to be unsuitable for ELISA development, a polyclonal antibody against rat VEGF-C was developed in rabbits (antibody 4080; BioGenes Berlin). The procedure was similar to that described for soluble VEGFR-2 (Röckl et al., 1998). Briefly, a total amount of 1.2 mg rat VEGF-C (containing a C-terminal 6His-tag) was used for immunization of two New Zealand white rabbits. After immunisation with 0.1 mg protein, each rabbit was boosted on days 7,

14, 28, 56 and 84 with the same amount. The dilution of the serum for half maximal titer was 1:10,000. Total IgG from rabbit serum was isolated using HiTrap Protein A Sepharose columns (Amersham Bioscience, Freiburg). The anti-VEGF-D antibody 4292 has been described previously (Kirkin et al., 2001).

2.2. Generations of cell lines, serum-free cell culture supernatants, lysates and tissue sample preparation

Experiments were conducted using three human (PC-3 cells, 293 cells, COLO 800 cells) and four rat (10AS, ARIP, BRL3A, MT-450) tumour cell lines. The COLO-800 cell line was purchased from DSMZ, Braunschweig. The PC-3, BRL3A and ARIP cell lines were maintained as monolayer cultures in Ham's F-12 medium (Flow Laboratories, Irvine, Scotland) at 37 °C in a humidified incubator with 5% CO_2. The 10AS and COLO-800 cell lines were cultured in RPMI-1640 medium (Gibco-BRL, Bethesda, MD). The wild type 293 and MT450 cell lines were cultured in DMEM medium. The 293 cells were co-transfected with a rat VEGF-C expression construct (Krishan et al., 2003) and a neomycin resistance vector using GenePORTER (Gene Therapy Systems). Stable transfected clones were selected and tested for VEGF-C expression and secretion using a polyclonal anti-VEGF-C antiserum (Kirkin et al., 2001). The transfected 293 cells were cultured in DMEM medium in the presence of neomycin. All medium was supplemented with 10% fetal bovine serum (Greiner, Germany).

The cells were grown to 80% confluence in 75-cm^2 tissue culture flasks (Nunc, Roskilde, Denmark). Conditioned media was collected under low-serum (2%) growth conditions. In some cases conditioned media was concentrated 10-fold by ultra-filtration using 10,000 Da cut-off membranes (Vivascience, Hannover, Germany). Tissues from transgenic RIP-Tag mice overexpressing mouse VEGF-C were a gift from Gerhard Christofori, Basel. Tissue lysates from different human tumours were either from the Metropolitan Komagome Hospital in Tokyo or from the Department of Pathology at the University of Kiel. All patients signed an informed consent according to a protocol approved by the ethics committees in each institute.

Tumour tissues were snap frozen in liquid nitrogen and homogenized in RIPA buffer (0.1% SDS, 1% IGEPAL CA-630, 0.5% Na-deoxycholate, protease-inhibitor cocktail in phosphate-buffered saline). Protein concentrations were estimated according to standard protocols (BCA assay, Pierce, Rockford).

2.3. Immunoblotting

Samples were loaded onto 12–15% sodium dodecyl sulphate polyacrylamide gel electrophoresis (SDS-PAGE) and separated under reducing conditions. Immunoblotting onto PVDF membrane (Millipore, Bedford, USA) was performed for 20 min at 15 V in a semi-dry blotting chamber. The membrane was blocked with 20% non-fat-milk in TBS (20 mM Tris–HCl, 150 mM NaCl, pH 8.0) for 1 h at room temperature. Antibody 4080 was used at 2 μg/ml IgG diluted in TBS containing 10% non-fat milk for 1 h at room temperature. The anti-VEGF-D antibody 4292 was used at 10 μg/ml IgG. The secondary antibodies and the ECL detection kit were used according to the instructions of the manufacturer (Amersham Bioscience, Freiburg).

2.4. VEGF-C sandwich-ELISA

The VEGF-C antibody 4080 was isolated from serum using HiTrap Protein-A Sepharose columns. Then, depletion of the anti-his antibody fraction was done by antigen-affinity purification using 10 mg of immobilized 6H-tagged TxnTb protein (Tryparedoxin (Txn) from *Trypanosoma brucei* (Tb)). Antigen-affinity purification for the antibody 4080 was performed by immobilising 1 mg rat VEGF-C on an NHS-activated HiTrap column (Amersham Bioscience, Freiburg). The development of a highly sensitive and specific sandwich ELISA for VEGF-C was done using standard methods (Harlow and Lane, 1988). Briefly, 10 μg/ml rabbit IgG 4080 was used for coating and the antigen-affinity purified and biotinylated antibody 4080 at 1 μg/ml was used as a detector antibody. Biotinylation of antibody 4080 was done with 6 mg IgG in 100 mM carbonate buffer, pH 8.5 at 3 mg/ml with using biotin-amidohexanoic acid NHS (Sigma, St. Louis, USA). The molecular ratio biotin:protein was 30:1. As a standard, human and rat dNdC-VEGF-C was used over a concentration range

between 0.1 and 6.25 ng/ml. For visualisation of the detector, streptavidin-enzyme conjugate was used (Endogen, Woburn, MA) followed by the addition of TMB (tetra-methyl-benzidine; Roche Mannheim, Germany). After stopping the reaction with 1 M H_2SO_4, the absorbance was measured at 450 and 620 nm with an ELISA plate reader (Labsystems, Finland). Generally, the samples were analyzed in different dilutions, measuring each dilution in duplicate. Samples were diluted at least 1/2 diluted with sample diluent (BenderMedSystems, Vienna).

2.5. RNA preparation, Northern blotting and PCR

Polyadenylated RNA was prepared from snap-frozen rat multiple tissues. Then, Northern blots using 1% agarose/formaldehyde gels and 5 μg polyadenylated RNA were performed as previously described (Hoffmann et al., 1998). Blots were performed at high stringency using VEGF-C (partial rat VEGF-C cDNA sequence, GenBank accession No. AF10302) for Northern blots of RNA from multiple tissue types. RNA gels were therefore stained with ethidium bromide and gels were inspected under UV light before and after Northern transfer to ensure that equivalent RNA was present in each lane.

2.6. RNA isolation for reverse transcription polymerase chain reaction (RT-PCR) analysis

Total RNA was extracted from the cells with TRIzol (Life Technologies, Grand Island, NY) according to the manufacturer's protocol. cDNAs were prepared using 5 μg of total RNA and Superscript II reverse transcriptase (Gibco-BRL) with oligo $(dT)_{12-18}$ primers and kept frozen at −80 °C until use. The resulting cDNAs were used to amplify the VEGF-C and β-actin using 5′ and 3′ primers and Taq polymerase (Invitrogen). The 5′ and 3′ primers for human VEGF-C was 5′-AGACTCAATGCATGCCACG-3′ and 5′-TTGAGTCATCTCCAGCATCC-3′, respectively, and those for β-actin were 5′-ATCTCCTTCTGCATCCTGTC-3′ and 5′-GACGAGGCCCAGAGCAAGAG-3′, respectively.

The conditions for the PCR were as follows: 95 °C for 5 min, 32 cycles of 30 s at 95 °C, 30 s at 53 °C, and 45 s at 72 °C, followed by a 10-min extension step at 72 °C for VEGF-C, and 94 °C for 2 min, 30 cycles of 20 s at 94 °C, 20 s at 57 °C, and 30 s at 72 °C, followed by a 10-min extension step at 72 °C for β-actin. The number of cycles in the RT-PCR was determined to yield a logarithmic range of amplification of each gene for semi-quantitative analysis of the expression levels of the two genes. The plasmid pCRII with the human VEGF-C cDNA was used as a positive control (Joukov et al., 1996). The RT-PCR

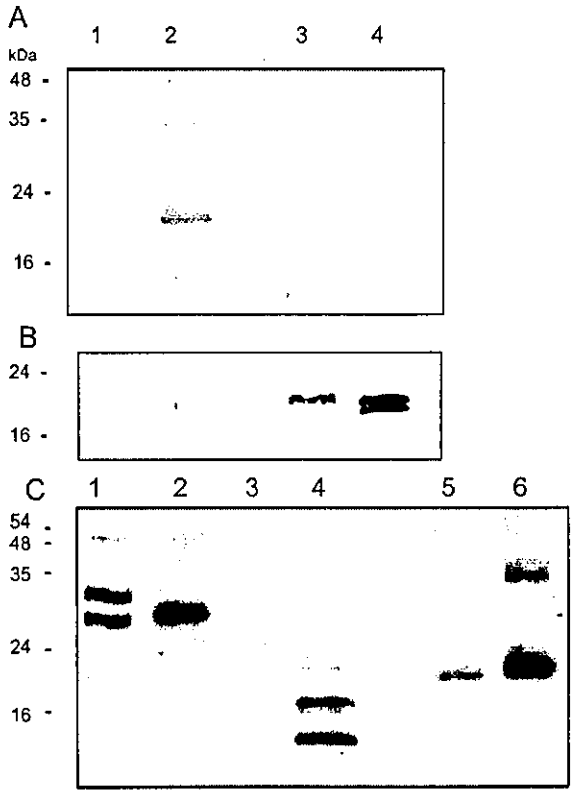

Fig. 1. Immunoblot with human and rat VEGF-C and VEGF-D using the polyclonal VEGF-C antibody 4080/his-depleted (A and C) and the anti-VEGF-D antibody 4292 (B). Proteins were separated by 12–15% SDS-PAGE and blotted on to PVDF membranes as described. After saturation, the membrane was incubated for 1 h with the AB 4080/his-depleted at 1–2 mg/ml in TBS containing 20% non-fat milk followed by incubation with a goat-anti-rabbit alkaline phosphatase-conjugated secondary antibody. A and B: Lane 1: 250 ng rat VEGF-C; lane 2: 250 ng human VEGF-C; lane 3: 250 ng rat VEGF-D; lane 4: 250 ng human VEGF-D. C: Lane 1: 150 μl 293 cell/VEGF-C supernatant; lane 2: 50 μg RIP TAG tumour lysate; lane 3: 10 μg insect cell lysate: lane 4: 10 μg rVEGF-C insect cell lyste; lane 5: 50 ng dNdC-rat VEGF-C; lane 6: 50 ng dNdC-human VEGF-C.

products were analysed by 2% agarose gel electrophoresis with ethidium bromide and documented.

3. Results

3.1. Characterization of the anti-VEGF-C polyclonal antibodies

First approaches to develop a VEGF-C ELISA were based on the use of commercially available antibodies but a satisfying antibody pair could not be selected. For this reason, we produced a polyclonal antibody in rabbits using the fully processed form of recombinant rat VEGF-C for the immunization. The serum was further purified by Protein A chromatography and by antigen-affinity purification to obtain pure rabbit IgG. Immunoblot analysis with human and rat VEGF-C and VEGF-D revealed that the antibody 4080 was specific for human and rat VEGF-C. Both proteins were recognized with similar sensitivities (Fig. 1A). This antibody showed no cross-reactivity with human and rat VEGF-D (Fig. 1B), the most closely related proteins to VEGF-C. Immunoblot analysis of VEGF-C containing tissues and secreting cells demonstrated that the antibody 4080 was able to recognize all forms of the molecule. Supernatants from rat VEGF-C transfected 293 cells exhibited three bands, most likely different glycosylated and processed forms of the mouse protein (Fig. 1C). In the transgenic RIP Tag mouse tumour overexpressing VEGF-C, only one band at 28 kDa could be detected in tissue lysates, indicating that fully processed forms were not generated in this model (Fig. 1C). Baculovirus-infected insect cell lysates contained unglycosylated and glycosylated forms of processed rat VEGF-C (dNdC-VEGF-C). The human fully processed VEGF-C from *Pichia pastoris* contained a main band at 22 kDa and a second band of 35 kDa (Fig. 1C).

3.2. Sensitivity, cross-reactivity and reproducibility of the sandwich ELISA for VEGF-C

Surprisingly, a substantial part of the antiserum was cross-reactive with the C-terminal 6H-tag of the antigen. Therefore, his-tag depletion by antigen-affinity chromatography significantly reduced the

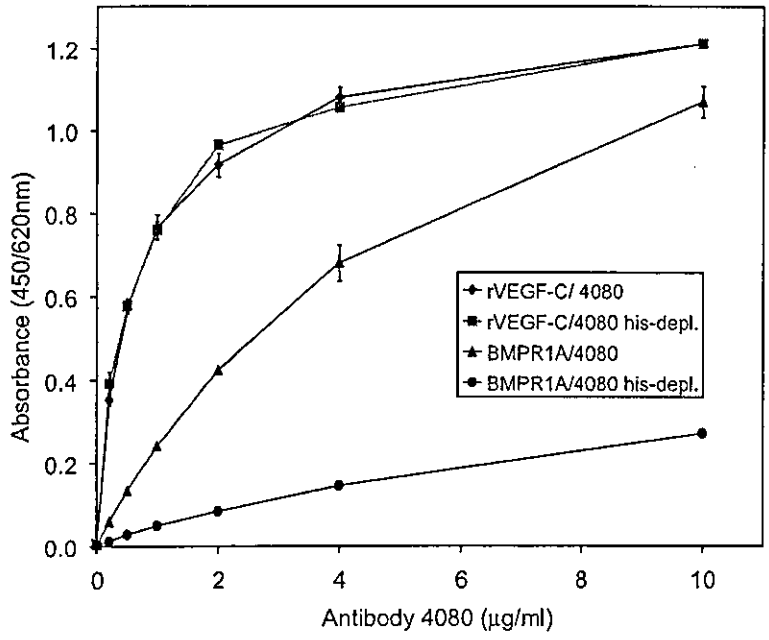

Fig. 2. Cross-reactivity of the 4080 antibody with VEGF-C and his-tagged proteins after anti-his-tag depletion. Rat VEGF-C and a unrelated his-tagged protein (BMPR1A) were coated at 2.5 µg/ml and detected by an increasing amount of the 4080 antibody before and after his-tag depletion as described. All measurements were performed in duplicate. Results show the mean absorbance at 450 nm as mean values.

cross-reactivity with other his-tag proteins, without modifying the affinity of the antiserum for VEGF-C (Fig. 2). The same polyclonal antibody 4080 was used as both capture and detector antibody and recognized different epitopes of the native, fully processed protein. The detector antibody was additionally antigen-affinity purified and biotinylated. This combination resulted in the most sensitive ELISA. A typical standard curve obtained with the ELISA is shown in Fig. 3. The minimum detection limit estimated by serial dilution was about 50 pg/ml of recombinant human and rat VEGF-C. Human VEGF-C was less readily detected than rat VEGF-C but this could be overcome by a threefold elongated incubation during colour development. If the sensitivity of the assay was determined as a significant difference from zero (two S.D. differences from the mean of the blank) using the data from Fig. 3, we calculated for rat VEGF-C a value of 6.9 pg/ml and for human VEGF-C a value of 54.5 pg/ml. As expected, VEGF-D was not recognized (Fig. 3). We also analysed the less closely related proteins VEGF-A, PlGF-1 and PlGF-2 for cross-reactivity and could not detect any significant binding (data not shown). To estimate the precision and reproducibility of the ELISA, intra-assay variations were evaluated. Supernatant from VEGF-C transfected 293 cells containing 2 ng/ml endogenous VEGF-C was spiked with recombinant rat VEGF-C to final concentrations of 4, 6 and 8 ng/ml, respectively. Intra-assay variations were estimated by duplicate measurements and at least 5 independent experiments. The intra-assay coefficients of variation (CV) were below 6% (Table 1).

Table 1
Intra-assay variations in cell supernatant samples assayed for VEGF-C

Sample	*n*	Mean (ng/ml)	SD	CV
1	6	2.005	0.176	8.75
2	5	4.004	0.119	2.99
3	5	5.646	0.250	4.43
4	5	8.371	0.482	5.76
Mean				5.48

Supernatants from 293/VEGF-C cells containing 2 ng/ml VEGF-C (sample 1) were spiked with 2 (2), 4 (3) and 6 (4) ng/ml recombinant VEGF-C.

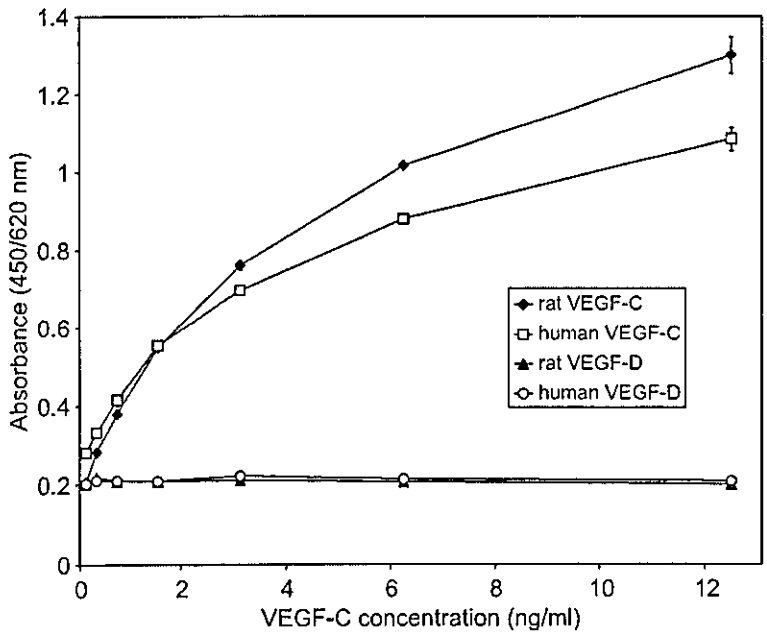

Fig. 3. Human and rat VEGF-C standard curves and cross-reactivity with the related protein VEGF-D. The different human and rat VEGF-C and -D preparations were diluted in assay buffer up to 12.5 ng/ml and a typical standard curve was measured using the ELISA procedure described. All measurements were performed in duplicate. The results show the absorbance at 450 nm as mean values. Rat VEGF-C standard was developed for 10 min, all other standards and controls for 25 min.

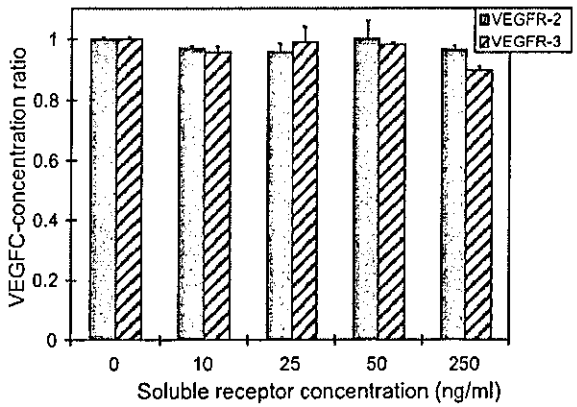

Fig. 4. Antibody 4080 binds to rat VEGF-C independenly of receptor-ligand complex formation. VEGF-C (6.25 ng/ml) was added to each well coated with AB 4080 in the absence or presence of increasing concentrations of soluble VEGFR-2 and VEGFR-3 preincubated with the ligand. Biotinylated 4080 antibody was used to detect and quantify bound VEGF-C. All measurements were performed and duplicate. Results show the mean absorbance at 450 nm as mean values.

In order to exclude interactions between VEGF-C/VEGFR-3 orVEGF-C/VEGFR-2 and VEGF-C/AB 4080 binding, increasing amounts of the corresponding soluble receptors were added to VEGF-C containing supernatants. As demonstrated in Fig. 5, a 15-fold excess of either of soluble VEGFRs did not interfere with the binding of 6.25 ng/ml VEGF-C to the capture antibody. This indicated that VEGF-C/VEGFR-3 or VEGF-C/VEGFR-2 complex formation did not adversely affect this assay (Fig. 4).

3.3. Secretion of VEGF-C from tumour cells and transfected cells under culture conditions

So far there is only limited information available about the kinetics and the amounts of VEGF-C secreted from cultured cells. Most of our knowledge about VEGF-C expression is based on gene expression studies made by Northern blot analysis and RT-PCR experiments. The rat tumour cell line BRL3A was chosen because of its relatively high expression of VEGF-C by Northern blot analysis (Krishan et al., 2003). Human 293 cells are chosen by many groups for transfection studies because they are well characterized, easy to transfect and good producers of many proteins. Although BRL3A cells express VEGF-C mRNA at a relatively high expression rate, only minor amounts of protein were secreted by these cells. After 6 days in culture only levels up to 80 pg/ml could be measured (Fig. 5). The low secretion rate of VEGF-C from other rat tumour cell lines in vitro was also noted (data not shown). However, transfected 293 cells secreted up to

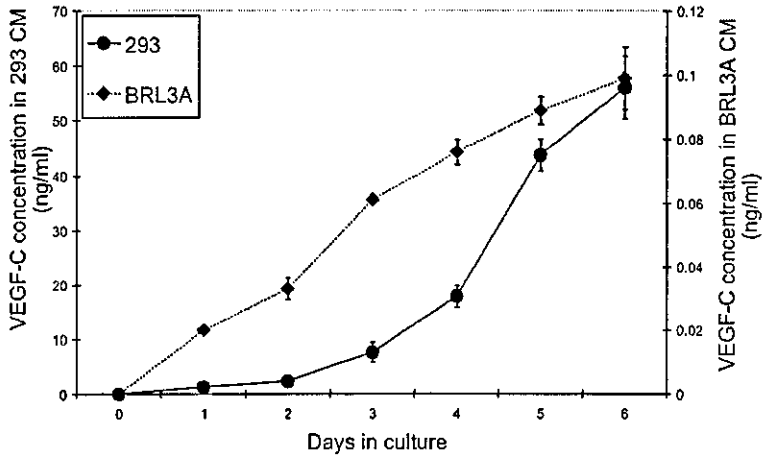

Fig. 5. Time course experiment for the secretion of rat VEGF-C from 293 cells transfected with the rat VEGF-C gene and from rat tumour BRL3A cells. Cells were cultured in 6-well plates over 1–6 days under normal culture conditions. Supernatants were collected and frozen at −20 °C before measurement and supernatant from BRL3A cells was concentrated before measurement. All measurements are done in duplicate and the mean values are indicated.

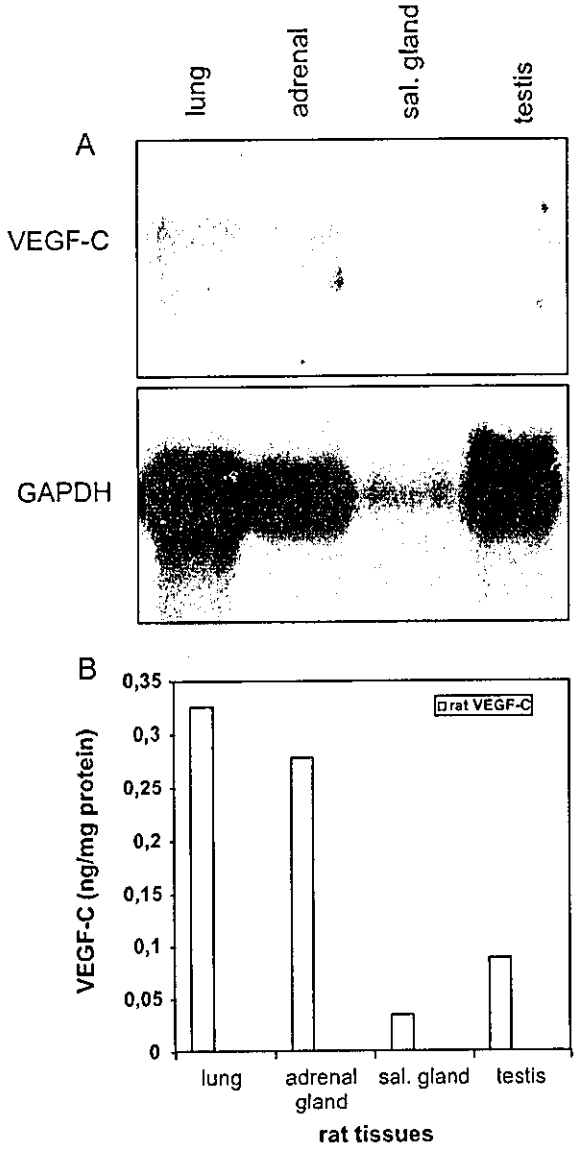

Fig. 6. Expression of VEGF-C in different rat tissues. (A) Northern blot analysis in a panel of polyadenylated RNAs derived from various rat tissues: lung, testis, salivary gland and adrenal gland. (B) ELISA measurements in samples prepared from the same rat tissues. Concentrations of rat VEGF-C are expressed as ng per mg of total protein.

50 ng/ml VEGF-C after 6 days of culture (Fig. 5). These results indicate that human 293 cells can secrete recombinant VEGF-C in relatively high amounts and that several molecular forms can be distinguished by immunoblot analysis (Fig. 1C).

3.4. Detection and quantification of VEGF-C from different murine and human tissues and correlation of VEGF-C data by using different detection methods

After the discovery of the VEGFR-3/Flt-4 ligand VEGF-C, several studies reported the expression of this gene in several tissues and organs of both human or murine origin (Joukov et al., 1996; Fitz et al., 1997; Kirkin et al., 2001). All of these studies used Northern blot analysis for the detection of human, mouse and rat VEGF-C. For the validation of our assay and to facilitate correlations with gene expression data we compared four rat tissues that are known either to express the VEGF-C gene at relatively high rates (lung and adrenal gland) or at relatively low rates such as testis and salivary gland (Kirkin et al., 2001). As shown in Fig. 6, ELISA measurements for the four different tissue lysates correlated with the Northern blot data also performed on the same (Fig. 6A and B). In 1 mg of total tissue protein, we could measure VEGF-C over the range 0.03–0.32 ng, indicating a very low abundance for VEGF-C in normal tissues. In further control experiments, we used RT-PCR with a primer pair specific for human VEGF-C. The human cDNA for VEGF-C was used as a positive control. Human PC-3 cells have been reported to exhibit high expression of VEGF-C (Joukov et al., 1996) and RT-PCR with our primer pair was able to confirm the expression of this gene (Fig. 7). On the other hand, the well characterized and frequently used human 293 cells expressed the

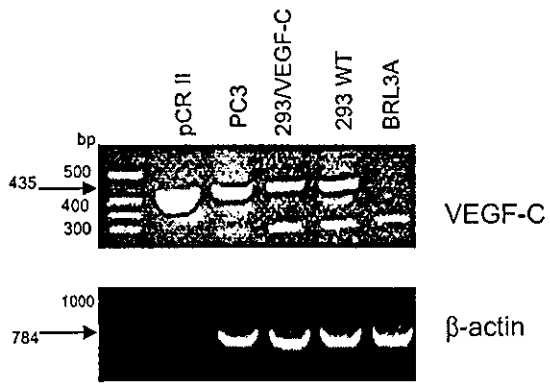

Fig. 7. Semi-quantitative RT-PCR analysis of human VEGF-C and β-actin in human and rat cancer cell lines. The sizes expected from the reported cDNA sequence for VEGF-C and β-actin are 435 and 784 bp, respectively.

gene at lower levels whether or not transfected with rat VEGF-C (Fig. 7). Because human specific PCR primers were used, the rat VEG-C gene could not be detected in transfected 293 cells nor in the BRL3A tumour cells (Fig. 7). Our ELISA measurements with PC-3 cells and 293 wild type cells were able to confirm the results. PC-3 cells have a high VEGF-C content in their lysates (Table 2), and untransfected human 293 cells exhibited a lower expression level. In lysates from 293 cells transfected with the rat VEGF-C gene, up to 7 ng of VEGF-C per mg total protein could be detected (Table 2). Several rat tumour cell lines have been characterized previously for VEGF-C expression (Krishan et al., 2003). These cell lysates were positive for VEGF-C but contained less VEGF-C than did PC-3 cells (Table 2). Samples from the control tumour cell line MT450 (Krishan et al., 2003) were also shown to have very low VEGF-C concentrations in their lysates. Many human tumours have been characterized over the last 6 years for VEGF-C gene expression but it is not yet clear how VEGF-C and its different processed forms participate in tumour angiogenesis and lymphangiogenesis. When we measured several human carcinoma lysates from different sources, we found concentrations in the range of 0.6–2.2 ng/mg protein of VEGF-C (Table 2). This is comparable to other cell lysates but lower than VEGF-A in breast cancer lysates (Toi et al., 2002). However, this information is based on a very limited number of tissues. Human lymph node tissue is also a good source of VEGF-C and preliminary experiments show that VEGF-C concentrations may be higher than in several other samples (Table 2).

Table 2
Quantification of VEGF-C in different cell culture samples and in tissue samples of different origin

Sample	*n*	Mean (ng/mg protein)	SD (%)
1. 293 cells/rVEGF-C SN (6 days)	4	11.84 (ng/ml)	0.085
2. 293 cells/rVEGF-C lysate	8	6.8	2.02
3. 293 cells/ WT lysate	2	0.43	0.131
4. BRL3A lysate	2	1.01	0.157
5. 10AS lysate	2	1.44	0.022
6. ARIP lysate	2	2.34	0.299
7. MT450 (negative control)	2	0.08	0.011
6. RipVEGF-C transgenic tumors	4	1.158	0.416
7. PC-3 cell lysate	8	6.85	2.528
8. Hum lymph node tissue	2	2.38	0.211
9. Breast cancer lysate	2	0.61	0.07
10. Pancreas cancer lysate 12,141	2	1.95	0.132
11. Gastric cancer lysate 19,907	2	2.20	0.141
12. Colon cancer lysate 2379	2	1.54	0.139

Samples were prepared from low serum containing media, cultured cells and from mouse and human tumour tissue and normal tissue samples. Cells were grown near confluency before being used for lysate preparation. Tumour samples were directly snap frozen after collection and homogenized in lysis buffer containing protease inhibitors. The VEGF-C concentrations were normalized at the concentration of the total protein in the lysate.

4. Discussion

The present study describes for the first time the establishment of a quantitative sandwich ELISA for murine and human VEGF-C. During the development of this ELISA, several polyclonal antibodies for VEGF-C were produced together with recombinant proteins for rat VEGF-C and VEGF-D. However, this approach was only successful because it was possible to use an antigen-affinity purified antibody against processed VEGF-C. Other antibodies such as anti-peptide antibodies or commercially available sources could not be used or were not sensitive enough for such an ELISA procedure.

In contrast to the other members of the VEGF family, VEGF-C and VEGF-D are produced as large precursor molecules and then processed during the release and secretion pathway (Joukov et al., 1997a,b). The largest monomeric unprocessed form is the 58 kDa protein. During the proteolytic processing of VEGF-C by proteases, major bands are seen at 30 kDa and 21 kDa in human PC-3 cells. The mature VEGF-C is the 21 kDa form but this cannot be detected in all VEGF-C producing cells and it is not clear if (partially) unprocessed forms can be secreted (Joukov et al., 1996, 1997a,b).

The antigen we have used was the rat processed VEGF-C (dNdC-VEGF-C) with a high degree of homology to mouse and human mature and processed VEGF-C. Mouse and rat VEGF-C show 100% sequence identity and between rat and human there is only one amino acid difference (Kirkin et al., 2001). Therefore, human and rat processed VEGF-C protein could be easily detected in our assay as well as by immunoblotting. However, when using our antibody

combination against the mature protein we cannot be certain that all VEGF-C forms are equally well detected in the assay. Using the lysate from the RIP Tag mouse tumour, we have some preliminary results that the 30 kDa protein may be less readily detectable than the 21 kDa protein.

Very recently, an ELISA for human VEGF-C has been reported (Duff et al., 2003). This ELISA used two polyclonal antibodies raised in a goat or in rabbits using the *Escherichia coli*-derived human VEGF-C peptide and a synthetic peptide corresponding to the C-terminal end of human the VEGF-C precursor. Therefore the assay recognizes the central VEGF-homology domain and carboxyl terminal domains of VEGF-C. With this ELISA, it was not possible to measure mature VEGF-C. Nor was it possible to include a dose–response curve with a recombinant VEGF-C. By immunoblotting using one or both antibodies the authors could demonstrate that plasma contained two immunoreactive 40 and 80 kDa proteins (Duff et al., 2003). From these studies it was not clear whether the two detected protein bands represented VEGF-C or other proteins cross-reacting with the antibodies. So far, 40 and 80 kDa VEGF-C proteins have not been described and mature VEGF-C could not be detected. Using plasma samples from patients with colorectal cancer, the authors could measure a threefold increase of VEGF-C in plasma. This would imply that unprocessed or partially processed forms of VEGF-C may be present in plasma samples from cancer patients. In our experiments we were not able to detect a 40 or 80 kDa band as putative unprocessed forms of VEGF-C. As discussed before, our antibody 4080 was made against the processed VEGF-C protein so that we cannot exclude the possibility that unprocessed, larger, precursor forms may not be detected. However, this is not very likely because at least partially processed forms can be detected in the RIP tag tumour mouse lysate (Fig. 1C).

We also assayed several plasma samples and found VEGF-C in some samples (data not shown). In cell and tissue lysates we were able to measure VEGF-C in relatively low amounts. Only transfected cells or PC-3 cells showed high levels of VEGF-C. Several reports in the last 6 years have claimed that many tumours express the VEGF-C or VEGF-D genes (Valtola et al., 1999; Stacker et al., 2001). With the exception of a few studies using antibodies to detect VEGF-C, most investigators have used RT-PCR or Northern blot procedures. Our study with human tumour samples suggests that the level of VEGF-C can be slightly lower than that of VEGF concentrations, e.g. VEGF-A in breast tumour samples (Toi et al., 2002). However, these results are the first ELISA data from tumour samples and further investigations are necessary to confirm our results. The pathophysiological significance of these findings remains unclear at present and it is also not known in which way VEGF-C contributes to tumour angiogenesis, lymphangiogenesis, tumour progression and metastasis.

From the early beginnings of VEGF-C research, PC-3 cells were described as high producers of VEGF-C (Joukov et al., 1996). Compared to tumour cells, these cells generate much more VEGF-C in lysates. It was surprising that the amount of VEGF-C in conditioned media and in corresponding cell lysates did not always correlate in our assays. It may suggest that only small amounts of VEGF-C are processed and secreted from cells under culture conditions. Further studies are necessary to confirm these more preliminary results and to investigate what are the reasons for the low and differing secretion rates in cell culture.

Acknowledgements

We are grateful to Drs Gerhard Christofori for RipTag mouse tumour tissue and Leopold Flohé for the TxnTb-6H protein for depletion experiments. Part of this work was supported by grants from the Deutsche Forschungsgemeinschaft to H.A.W. and J.P.S. under the auspices of Schwerpunktprogramm 1069 (Angiogenesis). Dr. Hiroko Bando is supported by a fellowship from the International Union Against Cancer (UICC).

References

Achen, M.G., Jeltsch, M., Kukk, E., Makinen, T., Vitali, A., Wilks, A.F., Alitalo, K., Stacker, S.A., 1998. Vascular endothelial growth factor D (VEGF-D) is a ligand for the tyrosine kinase VEGF receptor 2 (FLK) and VEGF receptor 3 (Flt4). Proc. Natl. Acad. Sci. U. S. A. 95, 548.

Duff, S.E., Li, C., Renehan, A., O'Dwyer, S.T., Kumar, S., 2003. Immunodetection and molecular forms of plasma vascular endothelial growth factor-C. Int. J. Oncol. 22, 339.

Fitz, L.J., Morris, J.C., Towler, P., Long, A., Burgess, P., Greco, R., Wang, J., Gassaway, R., Nickbarg, E., Kovacic, S., Ciarletta, A., Giannotti, J., Finnerty, H., Zollner, R., Beier, D.R., Leak, L.V., Turner, K.J., Wood, C.R., 1997. Characterization of murine Flt4 ligand/VEGF-C. Oncogene 15, 613.

Harlow, E., Lane, D., 1988. Antibodies: A Laboratory Manual Cold Spring Harbor Laboratory, New York.

Hoffmann, M., Fiber, C., Assmann, V., Gottlicher, M., Sleeman, J., Plug, R., Howells, N., von Stein, O., Ponta, H., Herrlich, P., 1998. Identification of IHABP, a 95 kDa intracellular hyaluronate binding protein. J. Cell. Sci. 111, 1673.

Hornig, C., Behn, T., Bartsch, W., Yayon, A., Weich, H.A., 1999. Detection and quantification of complexed and free soluble human vascular endothelial growth factor receptor-1 (sVEGFR-1) by ELISA. J. Immunol. Methods 226, 169.

Irrthum, A., Karkkainen, M.J., Devriendt, K., Alitalo, K., Vikkula, M., 2000. Congenital hereditary lymphedema caused by a mutation that inactivates VEGFR3 tyrosine kinase. Am. J. Hum. Genet. 76, 295.

Jeltsch, M., Kaipanen, A., Joukov, V., Meng, X., Lakso, M., Rauvala, H., Swartz, M., Fukumura, D., Jain, R.K., Alitalo, K., 1997. Hyperplasia of lymphatic vessels in VEGF-C transgenic mice. Science 276, 1423.

Joukov, V., Pajusola, K., Kaipainen, A., Chilov, D., Lahtinen, I., Kukk, E., Saksela, O., Kalkkinen, N., Alitalo, K., 1996. A novel vascular endothelial growth factor, VEGF-C, is a ligand for the Flt-4 (VEGFR-3) and KDR (VEGFR-2) receptor tyrosine kinases. EMBO J. 15, 290.

Joukov, V., Sorsa, T., Kumar, V., Jeltsch, M., Claesson-Welsh, L., Cao, Y., Saksela, O., Kalkkinen, N., Alitalo, K., 1997a. Proteolytic processing regulates receptor specifity and activity of VEGF-C. EMBO J. 16, 3898.

Joukov, V., Kaipainen, A., Jeltsch, M., Jajusola, K., Olofsson, B., Kumar, V., Eriksson, U., Alitalo, K., 1997b. Vascular endothelial growth factors VEGF-B and VEGF-C. J. Cell. Physiol. 1732, 211.

Junghans, B.M., Collin, H.B., 1989. Limbal lymphangiogenesis adter corneal injury: an autoradiographic study. Curr. Eye Res., 91.

Karkkainen, M.J., Ferrell, R.E., Lawrence, E.C., Kimak, M.A., Levinson, K.L., McTigue, M.A., Alitalo, K., Finegold, D.N., 2000. Missense mutations interfere with VEGFR-3 signalling in primary lymphoedema. Nat. Genet. 25, 153.

Kirkin, V., Mazitschek, R., Krishnan, J., Steffen, A., Waltenberger, J., Pepper, M.S., Giannis, A., Sleeman, J., 2001. Charakterization of indolinones which preferentially inhibit VEGF-C and VEGF-D-induced activation of VEFGFR-3 rather than VEGFR-2. Eur. J. Biochem. 268, 5530.

Korpelaionen, E.I., Alitalo, K., 1998. Signaling in angiogenesis and lymphangiogenesis. Curr. Opin. Cell Biol. 10, 159.

Krishan, J., Kirkin, V., Steffen, A., Heen, M., Weih, D., Tomarev, S., Wilting, J., Sleeman, J.P., 2003. Differential in vivo and in vitro expression of vascular endothelial growth factor (VEGF)-C and VEGF-D in tumors and its relationship to lymphatic metastasis in immunocompetent rats. Cancer Res. 63, 713.

Oh, S.J., Jeltsch, M.M., Birkenhaeger, R., McCarthy, J.E., Weich, H.A., Christ, B., Alitalo, K., Wilting, J., 1997. VEGF and VEGF-C specific induction of angiogenesis and lymphangiogenesis in the differentiated avian chorioallantoic membrane. Dev. Biol. 189, 96.

Pullinger, D., Florey, H., 1937. Proliferation of lymphatics in inflammation. J. Pathol. Bacteriol. 45, 157.

Röckl, W., Hecht, D., Sztajer, H., Waltenberger, J., Yayon, A., Weich, H.A., 1998. Differential binding characteristics and cellular inhibition by soluble forms of KDR and FLT-1. J. Exp. Cell Res. 241, 161.

Stacker, S.A., Stenvers, K., Caesar, C., Vitali, A., Domagala, T., Nice, E., Roufail, S., Simpsin, R.J., Moritz, R., Karpainen, T., Alitalo, K., Achen, M.G., 1999. Biosynthesis of vascular endothelial growth factor-D involves proteolytoic processing which generates non-covalent homodimers. J. Biol. Chem. 276, 32127.

Stacker, S.A., Caesar, C., Baldwin, M.E., Thornton, G.E., Williams, R.A., Preva, R., Jackson, D.G., Nishikawa, S.-I., Kubo, H., Achen, M.G., 2001. VEGF-D promotes the metastatic spread of tumor cells via the lymphatics. Nat. Med. 7, 186.

Toi, M., Bando, H., Ogawa, T., Muta, M., Hornig, C., Weich, H.A., 2002. Significance of vascular endothelial growth factor (VEGF)/soluble VEGF receptor-1 relationship in breast cancer. Int. J. Cancer 98, 14.

Valtola, R., Salven, P., Heikkila, P., Taipale, J., Joensuum, H., Rehn, M., Pihlajaniemi, T., Weich, H., deWaal, R., Alitalo, K., 1999. VEGFR-3 and its ligand VEGF-C are associated with angiogenesis in breast cancer. Am. J. Pathol. 154, 1381.

Veikkola, T., Jussila, L., Makinen, T., Karpanen, T., Jeltsch, M., Petrova, T.V., Kubo, H., Thurston, G., Mcdonal, D.M., Achen, M.G., Stacker, S.A., Alitalo, K., 2001. Signalling via vascular endothelial growth factor receptor-3 is sufficient for lymphangiogenesis in transgenic mice. EMBO J. 20, 1223.

Case Report

Oncology

Oncology 2004;67:476–479
DOI: 10.1159/000082933

Received: December 12, 2003
Accepted after revision: May 15, 2004

Germline Mutation of the LKB1/STK11 Gene with Loss of the Normal Allele in an Aggressive Breast Cancer of Peutz-Jeghers Syndrome

Chikashi Nakanishi[a] Tatsuro Yamaguchi[a] Takeru Iijima[c] Shigehira Saji[b]
Masakazu Toi[b] Takeo Mori[a] Michiko Miyaki[c]

[a]Department of Surgery, [b]Breast Oncology and Clinical Trial, and [c]Hereditary Tumor Research Project, Tokyo Metropolitan Komagome Hospital, Tokyo, Japan

Key Words
Breast cancer · Peutz-Jeghers syndrome · LKB1/STK11 gene

Abstract
Peutz-Jeghers syndrome (PJS) is an autosomal-dominant polyposis disorder with an increased risk of multiple cancer. The LKB1/STK11 gene, which acts as a tumor suppressor, is responsible for PJS and plays a role in suppressing breast cancer. The low expression of LKB1/STK11 in sporadic breast cancer is significantly associated with shorter survival. Here we describe a PJS patient with aggressive breast cancer that carried not only a germline mutation of LKB1/STK11 but also loss of the normal allele. The combination of these mutations may be associated with the poor prognosis of this patient. To our knowledge, we are the first to show that a germline mutation causing PJS is combined with the loss of the homologous normal allele of LKB1/STK11 in breast cancer.

Introduction

Peutz-Jeghers Syndrome (PJS) is an autosomal-dominant inherited disorder characterized by mucocutaneous pigmentation on the oral mucosa, lips and skin, and by multiple gastrointestinal polyps, mostly of the hamartomatous type. This syndrome is associated with malignant tumors in the gastrointestinal tract and elsewhere. The cumulative risk for breast cancer is 54% from 15 to 64 years old [1]. Recently, investigators discovered that a germline mutation of the LKB1/STK11 gene, a tumor suppressor gene on chromosome 19p3.3, causes this disorder [2–4].

Here we describe a case of significant progressive breast cancer with PJS, on which we carried out molecular analysis of the LKB1/STK11 gene mutation.

Case Report

A 41-year-old woman presented at our hospital on May 19, 2000, with right breast cancer diagnosed by fine needle aspiration cytology. A physical examination revealed a palpable, irregular hard mass of 4.2 × 4.0 cm in the right breast and a hard lymph node in the right axilla.

KARGER
Fax + 41 61 306 12 34
E-Mail karger@karger.ch
www.karger.com

0030–2414/04/0676–0476$21.00/0

Accessible online at:
www.karger.com/ocl

Chikashi Nakanishi
Department of Surgery, Tokyo Metropolitan Komagome Hp.
3-18-22 Honkomagome, Bunkyo-ku
113-8677 Tokyo (Japan)
Tel. +81 3 3823 2101, Fax +81 3 3824 1552, E-Mail chikashi-n@h3.dion.ne.jp

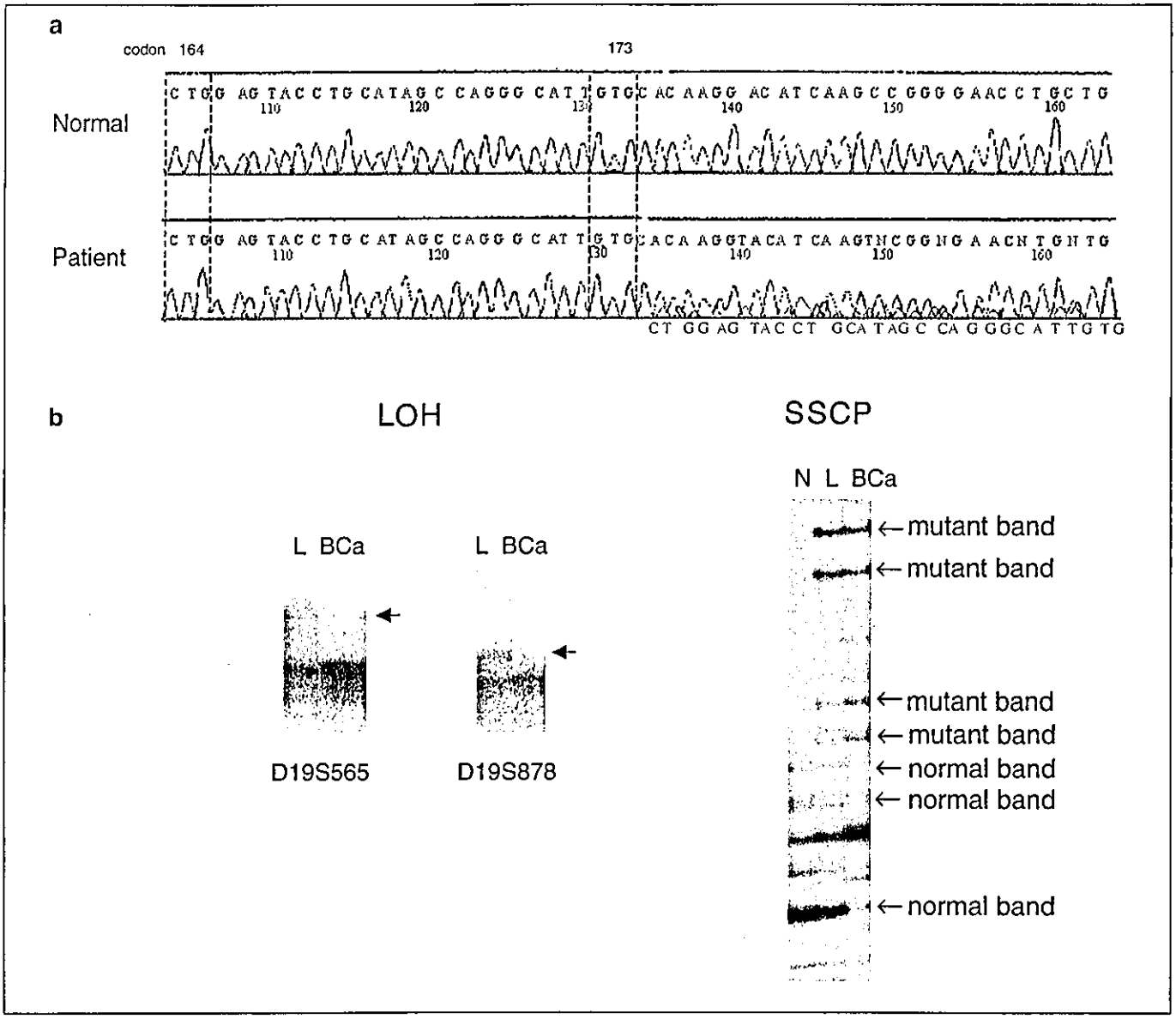

Fig. 1. a DNA sequence analysis of the LKB1/STK11 gene, using genomic DNA from peripheral lymphocytes. Exons 1–9 of the LKB1/STK11 gene in genomic DNA were analyzed by PCR-SSCP and then by direct sequencing of a particular exon exhibiting mutant bands. A germline mutation was detected in exon 4, 30-bp repeat from codons 164–173. **b** Loss of heterozygosity at the LKB1/STK11 locus, and the PCR-SSCP pattern of exon 4 of the LKB1/STK11 gene. LOH was analyzed by a microsatellite method using primers for the LKB1/STK11 locus. LOH was also detectable in PCR-SSCP of a specific exon showing mutant bands. The left panel indicates the loss of heterozygosity at the LKB1/STK11 locus in breast cancer tissues. The right panel shows the diminution of the normal band in the breast cancer sample. L = Lymphocyte; BCa = breast cancer.

Mammograms were performed and the right craniocaudal view showed an irregular mass 4.0 × 4.0 cm with obscured margins. Breast sonography showed a lobular hypoechoic mass with obscured margins in the right breast. Core-needle biopsy of the right breast tumor revealed an invasive ductal carcinoma.

In addition, mucocutaneous pigmentation was obvious on the lips and fingertips. The history of the patient and her family revealed that her son and grandfather had the same pigmentation, and that she had developed numerous colonic polyps during childhood. We suspected PJS and screening of the entire gastrointestinal tract revealed many hamartomatous polyps in the stomach and colon. The final diagnosis was, therefore, cancer of the right breast and PJS.

She received preoperative epirubicin and docetaxel therapy every 21 days, at a dose of 60 mg/m^2 for four courses. The clinical tumor

response was no response (cNR). The patient underwent breast conservation surgery with reconstruction using a latissimus dorsi flap on September 13, 2000. A histopathological examination revealed scirrhous breast carcinoma, whose pathological response to preoperative therapy was minor, with extensive lymphatic invasion. Nineteen of 22 lymph nodes examined involved tumors. An immunohistochemical test revealed that the breast cancer was negative for both estrogen and progesterone receptors as well as for HER2/neu.

We analyzed the mutation of the LKB1/STK11 gene in breast cancer and lymphatic cells using polymerase chain reaction-single strand conformation polymorphism and sequencing. We identified a germline mutation of the LKB1/STK11 gene in exon 4, which is a 30-bp repeat between codons 164 to 173 (fig. 1a). The normal LKB1/STK11 allele was lost in the breast cancer which was revealed by LOH analysis using D19S565 and D19S878, and by single strand conformation polymorphism analysis (fig. 1b).

Two more courses of adjuvant epirubicin and docetaxel therapy did not prevent the appearance of multiple bone and lymph node metastases in January 2001. The disease was essentially unresponsive to a combination of chemotherapy (paclitaxel, mitomycin, methotrexate), hormone therapy (medroxyprogesterone) and radiation therapy, and the patient died on June 3, 2001.

Discussion

PJS is an autosomal-dominant inherited disorder characterized by pigmented macules on the lips, perioral and buccal regions and by multiple gastrointestinal polyps mostly of the hamartomatous type. The association of mucocutaneous pigmentation with multiple gastrointestinal polyps was first described in 1921 by Peutz [5] who reported this association in several members of a family. In 1949, Jeghers et al. established the syndrome as an entity appearing to be inherited as an autosomal-dominant condition [6].

Patients with PJS are known to be at an increased risk for common gastrointestinal and nongastrointestinal cancers [1, 7–14]. The incidence of cancer among patients with PJS has been estimated to be 15- to 18-fold higher than in the general population [1, 3]. Giardiello et al. [1] reported that the cumulative risk from age 15 to 64 years for developing breast cancer in PJS patients was 54%.

Recently, investigators discovered that germline mutations of the LKB1/STK11 gene on chromosome 19p13.3 cause PJS [2, 3]. Gruber et al. [4] reported evidence that LKB1/STK11 acts as a tumor suppressor gene potentially involved in the earliest development of the pathogenesis of hamartomas into adenocarcinoma. As implied by Knudson's two-hit hypothesis [15], most cancer predisposition syndromes are caused by a mutation in a recessive tumor suppressor gene. When one allele is defective in the germline, the chance of complete inactivation of the gene by somatic loss of the remaining normal allele is dramatically increased. By this hypothesis, it is possible to speculate that cancers (including breast cancer) in PJS are caused by loss of the LKB1/STK11 gene function. A report of 31 sporadic breast cancers showed weak LKB1/STK11 expression in 9 cases [16]. Shen et al. [17] reported that LKB1/STK11 plays a role in the tumor suppressor function in sporadic breast cancer, and low expression of the LKB1/STK11 protein is significantly associated with a shorter survival. However, several attempts have failed to show the somatic mutation of LKB1/STK11 in breast cancer [18–20].

In our patient, we identified a germline mutation of the LKB1/STK11 gene. In addition, the loss of the normal LKB1/STK11 allele was detected in the breast cancer sample, but not in the peripheral leukocytes. It is, therefore, suggested that the total disability of the LKB1/STK11 gene may cause breast cancer. Thus, this case demonstrates Knudson's two-hit hypothesis. Furthermore, the prognosis was poor: the breast cancer recurrence was detected 4 months after surgery, and she died after 21 months.

To our knowledge, this is the first case showing the combination of a germline mutation of LKB1/STK11 and loss of the normal allele in breast cancer in a PJS patient. It is suggested that the combination of these mutations may have been related to cancer development and a significantly poor prognosis in this patient.

References

1 Giardiello FM, Brensinger JD, Tersmette AC, et al: Very high risk of cancer in familial Peutz-Jeghers syndrome. Gastroenterology 2000;119: 1447–1453.

2 Hemminki A, Markie D, Tomlinson I, et al: A serine/threonine kinase gene defect in Peutz-Jeghers syndrome. Nature 1998;391:184–187.

3 Jenne DE, Reimann H, Nezu J, et al: Peutz-Jeghers syndrome is caused by mutations in a novel serine threonine kinase. Nat Genet 1998; 18:38–43.

4 Gruber SB, Entius MM, Petersen GM, et al: Pathogenesis of adenocarcinoma in Peutz-Jeghers syndrome. Cancer Res 1998;58:5267–5270.

5 Peutz JLA: Over seen zeer merkwaardige gecombineerde familiare polyposis van den slymvliezen van den tractus intestinalis metdie van de neuskeelholte en gepaard met eigenaardge pigmentaties van huid en slijmvliezen. Ned Maandschrift Geneesk 1921;10:134–146.

6 Jeghers H, McKusick VA, Katz KH: Generalized intestinal polyposis and melanin spots of the oral mucosa, lips and digits: A syndrome of diagnostic significance. N Engl J Med 1949; 241:993–1005, 1031–1036.

7 Giardiello FM, Welsh SB, Offerhaus GJA, et al: Increased risk of cancer in Peutz-Jeghers syndrome. N Engl J Med 1987;316:1511–1514.

8 Hizawa K, Iida M, Matsumoto T, et al: Cancer in Peutz-Jeghers syndrome. Cancer 1993;72: 2777–2781.

9 Spigelman AD, Murday V, Phillips RKS: Cancer and the Peutz-Jeghers syndrome. Gut 1989; 30:1588–1590.

10 Westerman AM, Entius MM, van Velthuysen MLF, et al: Cancer risk in Peutz-Jeghers syndrome (abstract). Eur J Hepatogastroenterol 1998;10:A42.

11 Boardman LA, Thibodeau SN, Schaid DJ, et al: Increased risk for cancer in patients with the Peutz-Jeghers syndrome. Annal Intern Med 1998;128:896–899.

12 Foley TR, McGarrity TJ, Abt AB: Peutz-Jeghers syndrome: A clinicopathologic survey of the 'Harrisburg family' with a 49-year follow-up. Gastroenterology 1988;95:1535–1540.

13 Burdick D, Prior JT: Peutz-Jeghers syndrome: A clinicopathologic study of a large family with a 27-year follow-up. Cancer 1982;50:2139–2146.

14 Utsunomiya J, Gocho H, Miyanaga T, et al: Peutz-Jeghers syndrome: Its natural course and management. Johns Hopkins Med J 1975;136: 71–82.

15 Kundson AG: Hereditary cancer, oncogenes, and antioncogenes. Cancer Res 1985;45:1437–1443.

16 Andrew R, Micheal C: In situ analysis of LKB1/STK11 mRNA expression in human normal tissue and tumors. J Pathol 2000;192: 203–206.

17 Shen Z, Wen XF, Lan F, et al: The tumor suppressor gene LKB1 is associated with prognosis in human breast carcinoma. Clinical Cancer Res 2002;8:2085–2090.

18 Bignell GR, Barfoot R, Seal S, et al: Low frequency of somatic mutations in the LKB1/Peutz-Jeghers syndrome gene in sporadic breast cancer. Cancer Res 1998;58:1384–1386.

19 Foster LF, Defres S, Goudie DR, et al: An investigation of the Peutz-Jeghers gene (LKB1) in sporadic breast and colon cancer. J Clin Pathol 2000;53:791–793.

20 Chen J, Lindblom A: Germline mutation screening of the STK11/LKB1 gene in familial breast cancer with LOH on 19p. Clin Genet 2000;57:394–397.

A close association between alteration in growth kinetics by neoadjuvant chemotherapy and survival outcome in primary breast cancer

MASAHIRO TAKADA[1], AKEMI KATAOKA[3], MASAKAZU TOI[1], HIROKO BANDO[1], KAZUMI TOYAMA[1], SHINICHIRO HORIGUCHI[2], TAKAYUKI UENO[4], STIG LINDER[4], SHIGEHIRA SAJI[1], YUKIKO HAYASHI[2], NOBUAKI FUNATA[2], JUNKO KINOSHITA[3], SIGERU MURAKAMI[3] and SHINJI OHONO[3]

Departments of [1]Surgery, and [2]Pathology, Tokyo Metropolitan Komagome Hospital, 3-18-22 Honkomagome, Bunkyo-ku, Tokyo 113-8677; [3]Department of Breast Oncology, National Kyushu Cancer Center Hospital, 3-1-1 Notame, Minami-ku, Fukuoka 811-1395, Japan; [4]Cancer Center Karolinska, Department of Oncology and Pathology, Karolinska Institute and Hospital, Stockholm, S-171 76, Sweden

Received February 9, 2004; Accepted April 6, 2004

Abstract. Few surrogate markers are available for predicting the survival benefit from chemotherapy in primary breast cancer. We examined tumor growth kinetics by assessing cytokeratin 18 neo-epitope (CK18NE), an apoptosis marker detected by M30 antibody and Ki-67 antigen, a proliferation marker detected by MIB-1 antibody in 72 primary breast cancer patients who underwent pre-operative anthracycline-based chemotherapy. Increase in M30 index and decrease in MIB-1 index after the exposure of 2 to 4 cycles of chemotherapy correlated significantly with pathological tumor response. Univariate survival analysis, conducted in the subgroup of 42 patients who underwent CAF (cyclophosphamide, adriamycin and 5-FU) therapy alone, showed that the patients with the high levels of M30 index (>35 counts/1000 tumor cells) and the low levels of MIB-1 index (<140 counts/1000 tumor cells) after chemotherapy had a remarkably favorable prognosis as compared with patients in other categories. In addition, the alteration in growth kinetics by the treatment showed a significant prognostic value. Multivariate analysis also confirmed that the post-treatment growth kinetics was an independent prognostic indicator. These findings suggest that the alteration in growth kinetics revealed by CK18NE and MIB-1 might be a surrogate marker for predicting the survival benefit from chemotherapy in primary breast cancer.

Correspondence to: Dr Masakazu Toi, Tokyo Metropolitan Komagome Hospital, 3-18-22 Honkomagome, Bunkyo-ku, Tokyo 113-8677, Japan
E-mail: maktoi77@wa2.so-net.ne.jp

Abbreviations: ER, estrogen receptor; PgR, progesterone receptor; 5-FU, 5-fluorouracil; ADR, adriamycin; Epi, epirubicin; CPA, cyclophosphamide, pre-CT, pre-operative chemotherapy

Key words: cytokeratin 18, M30, preoperative chemotherapy, apoptosis, breast cancer

Introduction

Chemotherapy cures a certain population of cancer patients (1). For instance, post-operative adjuvant poly-chemotherapy provides a significant annual reduction in chances of recurrence for patients with primary breast cancer. Nevertheless, it is still difficult to predict the survival benefit from chemotherapy individually without long-term follow-up. Although several molecules such as the p53 mutation have been raised as a surrogate of chemotherapeutic effect, most of them were characterized as resistance markers rather than sensitive markers for chemotherapy (2,3).

Recently, the NSABP B-18 trial, investigating the clinical impact of pre-operative chemotherapy (pre-CT) using 4-cycles of adriamycin (ADR) plus cyclophosphamide (CPA) for primary breast cancer patients, showed that pathological complete response (pCR) was a potent prognostic indicator for favorable prognosis (4,5). Clinical response, even clinical CR, did not show any significant prognostic value for long-term outcome. Since other pre-CT studies using different types of chemotherapy regimens have also confirmed the prognostic significance of pCR, pCR is regarded as a surrogate marker for identifying the chemo-sensitive subpopulation in primary breast cancer (6).

In addition to pCR, various markers are tested currently to explore the surrogate value for long-term therapeutic benefit from chemotherapy, because it is estimated that a chemotherapy-sensitive subpopulation might exist in non-pCR group. We have studied the changes of tumor growth kinetics elicited by chemotherapy for a similar purpose. Among apoptosis markers, we focused on the neo-epitope of cytokeratin 18 (CK18NE), which often emerges with chemotherapy. It is known that structural changes of cells occur during apoptosis mediated by proteases such as those of

the caspase family, which cleave a number of intracellular substrates. One of these substrates, CK18 is a major component of intermediate filaments of simple epithelial cells and tumor cells derived from such cells, and it is cleaved into proteolytic fragments by caspases during apoptosis. Recently, a monoclonal antibody, M30 was generated to identify CK18NE, mapping to amino acids 387-396, exposed after caspase cleavage during apoptosis (7-9). The previous immunohistochemical studies confirmed that M30 recognizes apoptotic cells that show cytoplasmic staining, while it does not recognize viable and necrotic cells (7,10,11).

In the present study, we analyzed tumor growth kinetics using CK18NE and cell proliferation antigen Ki-67, detected by MIB-1 antibody, and examined its changes by pre-operative anthracycline-based chemotherapy in primary breast cancer patients. The results will indicate that the alteration in tumor growth kinetics by pre-operative chemotherapy is useful for assessing long-term therapeutic benefit from the chemotherapy in primary breast cancer.

Materials and methods

In vitro study. In order to confirm the induction of M30 by chemotherapy, we used MDA-MB-231, a hormone-independent human breast carcinoma cell line. The cells were grown in 96-well plates in 200 µl DMEM 10% FCS overnight, the medium changed, and then doxorubicin was added to 1 µg/ml. NP40 was added to the medium (final 0.5%) at the times indicated to assay total accumulated CK18-Asp396 (in living cells still attached + in dead cells + released activity in medium), and 25 µl was assayed by M30-Apoptosense™ enzyme-linked immunosorbent assay (ELISA) kit (PEVIVA, Bromma, Sweden). ELISA was conducted according to the manufacturer's instruction.

Patients and tumor materials. Seventy-two women receiving pre-CT for untreated breast cancer in the National Kyushu Cancer Hospital and the Komagome Metropolitan Hospital between December 1992 and December 1999 were enrolled. Clinico-pathological features of the patients enrolled are shown in Table I. Pairs of breast cancer samples were obtained before and after pre-CT by excisional biopsy and radical operation. Informed consent was obtained according to the procedures of each institute. Both biopsied and surgical resected samples were sufficient for accurate histological diagnosis, measurement of apoptosis, proliferation and biomarkers. Out of 72 patients, 49 were treated with FAC regimen, adriamycin (ADR) 40 mg/m^2 at day 1 and cyclophosphamide (CPA) 400 mg/m^2 and 5-FU 400 mg/m^2 at day 1 and day 8 repeated every 3 weeks (q3), 9 with CEF, CPA 600 mg/m^2, epirubicin (Epi) 60 mg/m^2, 5-FU 600 mg/m^2 q3, 7 with AC, ADR 60 mg/m^2 and CPA 600 mg/m^2 q3, and 7 with EC, Epi 75 mg/m^2 and CPA 600 mg/m^2 q3. All the patients were without distant metastasis at the time of diagnosis and received operations with axillary dissection. Clinico-pathological data and response to pre-CT are summarized in Table II. Response to pre-CT was established by clinical assessment of breast mass according to the criteria of International Union Against Cancer. Survival analysis was performed in a subgroup of 42 patients who underwent FAC therapy alone pre- and post-operatively. These

Table I. Clinico-pathological data and response to pre-operative chemotherapy.

No. of patients	72
Median age (years)	51 (28-74)
Menopause	
Pre-menopausal	33
Post-menopausal	39
Pre-tumor size	
T1, T2	9
T3	26
T4	37
Pre-nodal status	
N0	16
N1	29
N2	16
N3	10
Unknown	1
Histlogical subtype	
Invasive ductal carcinoma	66
Invasive lobular carcinoma	1
Unknown	5
Estrogen receptor	
Positive	44
Negative	28
Progesterone receptor	
Positive	32
Negative	40
Chemotherapy regimen	
FAC	49
CEF	9
AC	7
EC	7
No. of cycles of preoperative chemotherapy	
2 cycles	29
3 cycles	26
4 cycles	14
≥5 cycles	3
Clinical response to chemotherapy	
CR	2
PR	29
NC	39
PD	2
Post-chemotherapy size	
t1, t2	24
t3	17
t4	30
Unknown	1
Pathological response to chemotherapy	
0	18
1a	34
1b	12
2	7
3	1

FAC, 5-FU, adriamycin (Adr) and cyclophosphamide (CPA); CEF, CPA, epirubicin (Epi) and AC, Adr and CPA; EC, Epi and CPA. CR, complete response; PR, partial response defined as a >50% reduction rate; NC, no significant change; PD, progressive disease.

Table II. Relationship between clinico-pathological parameters and the status of M30 and MIB-1, and therapeutic response.

Factors	Clinical response NR vs R	Pathological response grade 0-1 vs grade 2-3	Pre M30 ≥35 vs <35	Pre MIB-1 ≥240 vs <240	Post M30 ≥35 vs <35	Post MIB-1 ≥240 vs <240
Menopausal status						
Negative vs positive	NS	NS	NS	NS	NS	NS
Pre-tumor size						
T0-T3 vs T4	NS	NS	NS	NS	NS	NS
Pre-nodal status						
N0-1 vs N2-3	NS	NS	NS	NS	NS	NS
Estrogen receptor						
Negative vs positive	NS	NS	NS	0.0018	NS	0.0021
Progesterone receptor						
Negative vs positive	0.0405	NS	NS	0.0069	NS	NS

NR, non-responder (NC + PD); R, responder (CR + PR); NS, not significant.

patients underwent operations after 2-4 cycles of FAC treatment and continued the same FAC treatment post-operatively until the full dose of antharacycline (500 mg/m^2). No patients received radiation therapy or endocrine therapy. Patients were followed-up at least at 3-month intervals, and recurrence was confirmed by histological examination or image examination. Twenty-five patients developed recurrence and 19 patients died of breast cancer within the follow-up period (median follow-up: 2.7 years when censored at relapse).

Evaluation of tumor response. Response of the primary tumors by chemotherapy was evaluated according to criteria established by the Japanese Breast Cancer Society, which are essentially the same as those of the World Health Organization. CR (complete response), is defined as the disappearance of tumor; PR (partial response), refers to a decrease in tumor size of ≥50%; NC (no change), indicates a decrease in tumor size of ≤50% or an increase of tumor size by <25%; PD (progressive disease), indicates an increase in tumor size of ≥25%.

The grading of the pathological efficiency by chemotherapy, which is evaluated by microscopic evaluation by a skilled pathologist, was also categorized according to the criteria established by the Japanese Breast Cancer Society. Grade 3, is defined as the complete disappearance of variable cancer cells on the examined specimens; grade 2, refers to apparent degeneration of 2/3 or more of the population of observed cancer cells; grade 1, indicates observation of degenerative cells in less than 2/3 of examined tumor cells; grade 0, indicates lack of findings of degenerative cancer cells on specimens.

Determination of conventional biological markers. All specimens, fixed in 10% formaldehyde solution and embedded in paraffin, were examined by conventional procedures to obtain a histological diagnosis. Estrogen receptor (ER) and progesterone receptor (PgR) levels were determined with ELISA systems from Otsuka Assay Institute (Tokushima, Japan) as reported previously, or by immunohistochemistry (12,13). The cut-off values for ER and PgR in biochemical assay were 13 fmol/mg protein and 10 fmol/mg protein, respectively. For immunohistochemical determination of ER and PgR, tumors containing 10% or more receptor-positive cells were regarded as receptor-positive status. Her-2 and p53 immunostainings were performed as previously described (12).

Tumor growth kinetics assessed by CK18NE and Ki-67 antigen. The 4 μm-thick sections, mounted on the silane-coated glass, were dewaxed in xylene, rehydrated through descending concentrations of alcohol, and treated with 0.3% hydrogen peroxide in methanol for 15 min to inhibit the endogenous peroxidase activity. The sections for MIB-1 staining were autoclave pre-treated for 15 min at 121°C in a solution of 10 mM citrate buffer (pH 6.0) and the section for M30 staining were pre-treated with pepsin solution (1 mg/ml in phosphate buffer) for 15 min at 37°C. The mouse monoclonal antibody M30 CytoDeath (Roche, Basel, Switzerland) against caspase-cleaved CK18NE was incubated with tissue sections at a 1:200 dilution for 30 min at room temperature. The mouse monoclonal antibody against Ki-67 (clone MIB-1; Dako, Glostrup, Denmark) was incubated with tissue sections at a 1:50 dilution for 1 h at room temperature. All of the slides were processed using the commercial Elite ABC kit (Vectastain, Vector Laboratories, Burlingame, CA) directed against mouse IgG. Diaminobenzidine was used as the final chromogen and Meyer's hematoxylin was used for counterstain.

At least 1000 neoplastic cells were analyzed by at least three different microscopic views in each case. The ratio of positively stained cells, cytoplasmic staining for M30 and nuclear staining for MIB-1, was counted and the M30 index and MIB-1 index were calculated as the average of these counts, respectively. All immunohistochemical stainings were evaluated without knowledge of clinical outcome. Two experienced pathologists independently confirmed the histological diagnosis of all specimens. Positive and negative controls were run in parallel.

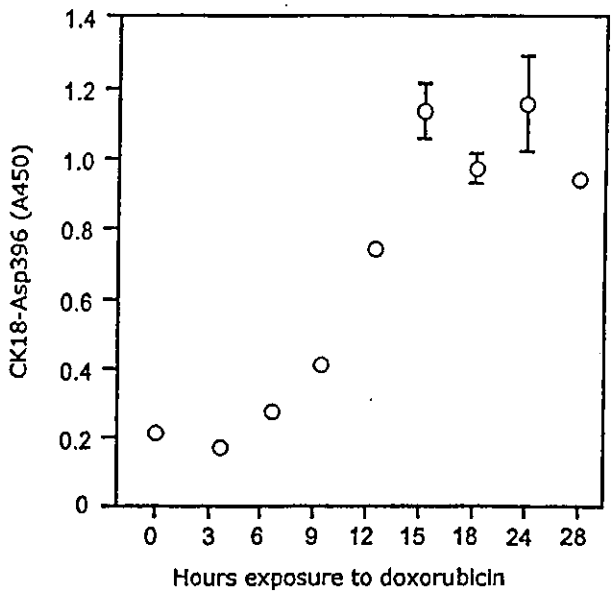

Figure 1. Increase of M30 by doxorubicin *in vitro*. A time-course experiment showing the increase of M30 by 1 μg/ml doxorubicin treatment in MDA-MB-231 cells. Each plot indicates the value of mean ± standard deviation (SD). Values which have minimum SD did not show the area of SD on the graph. A significant difference was observed between 0 and 15 h ($p>0.0001$, t-test).

Statistical analysis. The relationship between examined biomarkers and the clinical variables, including the clinico-pathological factors and treatment characteristics listed in Table I, were analyzed using the Chi-square test or Student's t-test. The relationship between M30 index and MIB-1 index was analyzed with the correlation test. The survival curves were plotted according to the Kaplan-Meier method, and the log-rank test was applied to compare the survival curves. Multivariate analyses were performed using the Cox proportional hazards model. All statistical tests were performed using the StatView software package (Abacus Concepts Inc.) and the findings were considered significant when the p-value was <0.05.

Results

Increase of M30 by doxorubicin in vitro. A time-course experiment showed that the M30 levels increased immediately after the exposure to doxorubicin in MDA-MB-231 cells. The increase from 0 to 15 h was statistically significant at the level of $p<0.0001$ by t-test (Fig. 1). This was also true for 18, 24 and 28 h.

M30 index and MIB-1 index. Pre-treatment M30 index ranged from 1 to 574 counts (median: 2.5 count/1000 neoplastic cells) and pre-treatment MIB-1 index ranged from 34 to 825 counts

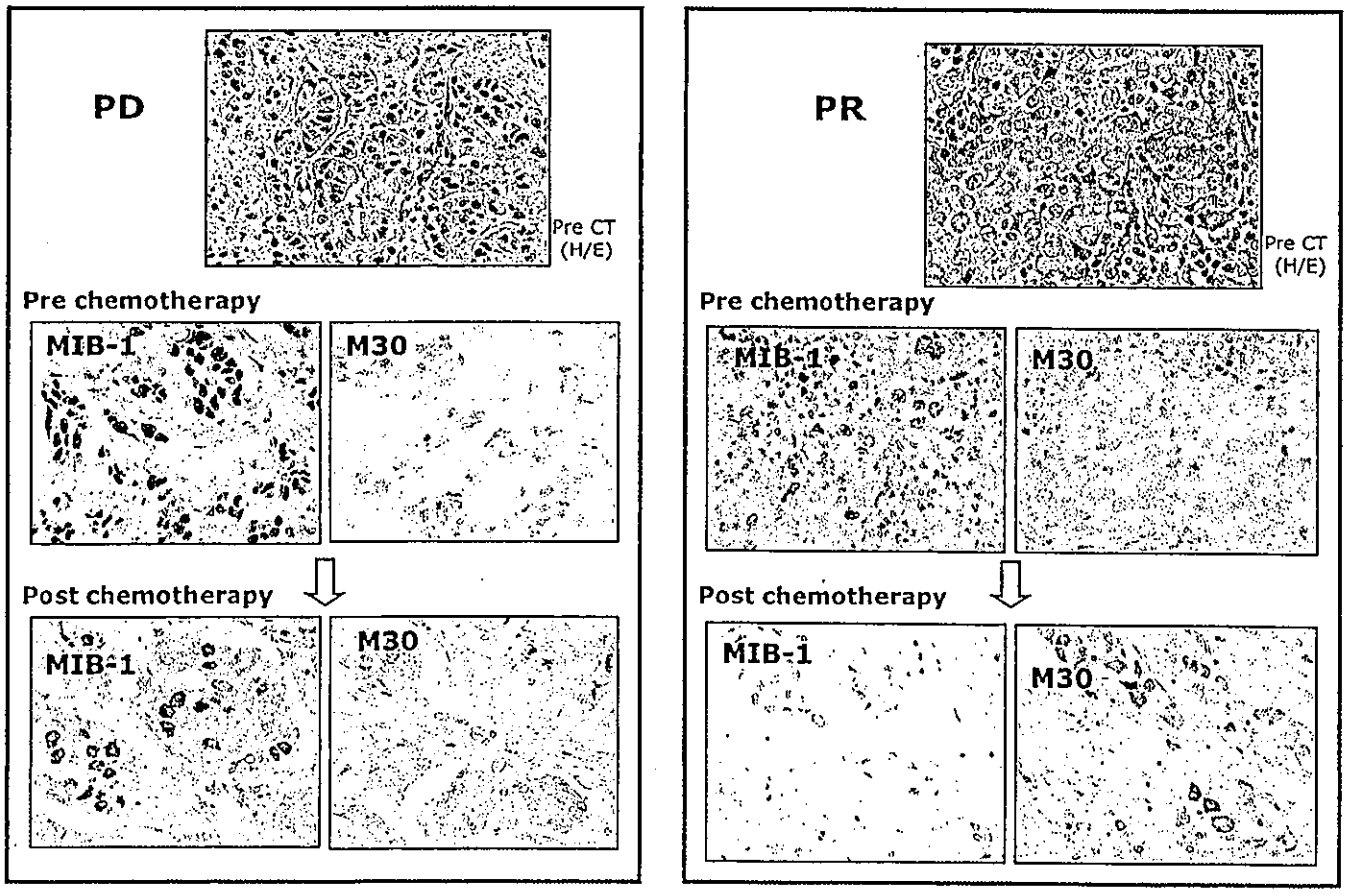

Figure 2. Representative staining of M30 and MIB-1 and the changes of growth kinetics by chemotherapy. Positive cytoplasmic staining was assessed as positive for M30, and positive nuclear staining was assessed as positive for MIB-1. M30 index and MIB-1 index were calculated as the positive cell rate of 1000 tumor cells. In non-responders (PD, clinically progressive disease), no decrease in MIB-1 index and no increase in M30 index were observed. In responders (PR, clinically partial response), MIB-1 index decreased significantly, and M30 index increased remarkably.

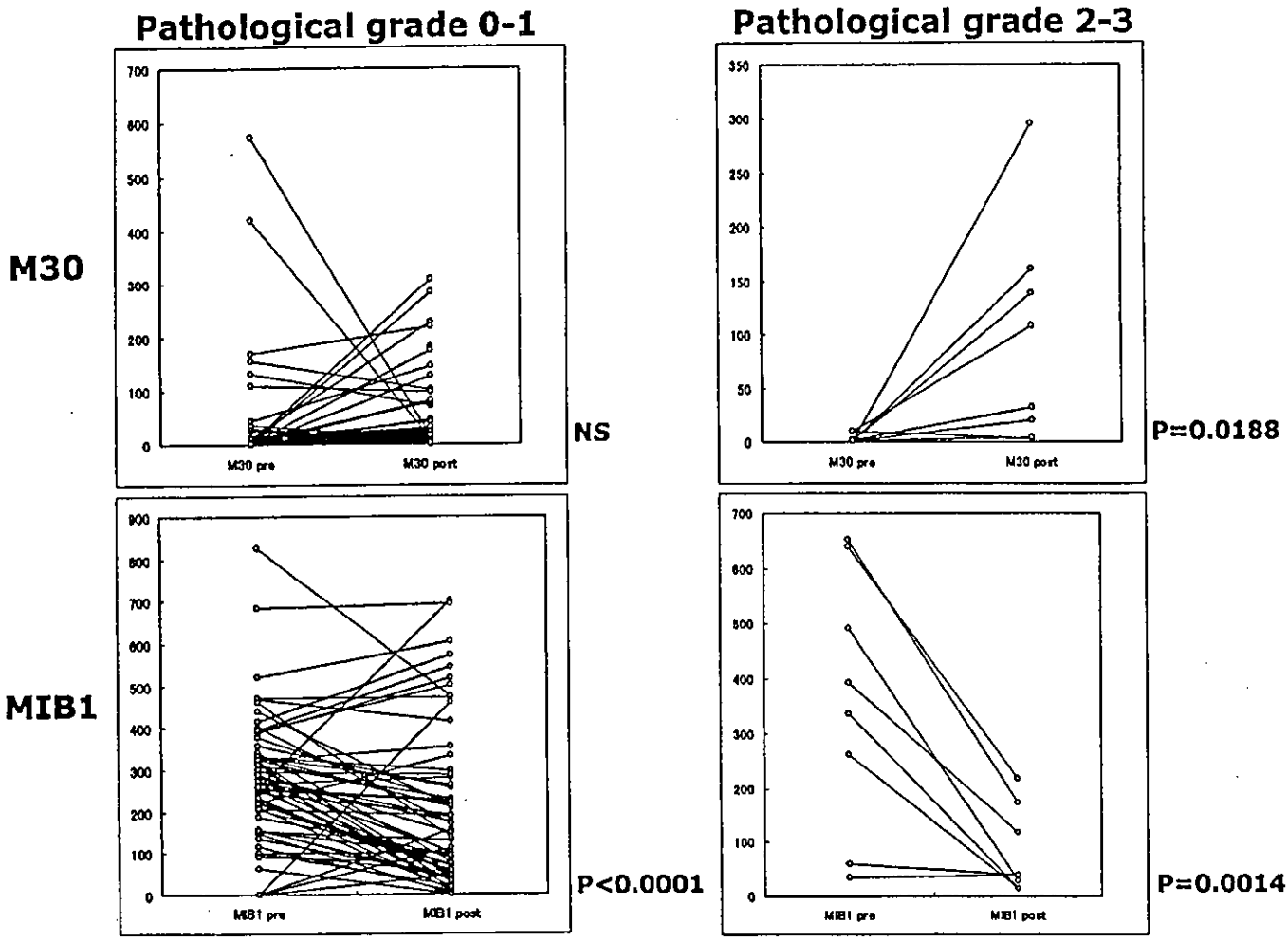

Figure 3. The relationship between the changes in M30 index and MIB-1 index and pathological response grade. The rules of Japanese Breast Cancer Society were used for assessing pathological tumor response (see Materials and methods). In pathological grade 2 patients, a significant increase in M30 index and a significant decrease in MIB-1 index were observed.

(median: 274 count/1000 neoplastic cells). Post-treatment M30 index ranged from 1 to 308 counts (median: 13 count/1000 neoplastic cells) and post-treatment MIB-1 index ranged from 1 to 701 counts (median: 124.5 count/1000 neoplastic cells). Representative cases of M30 and MIB-1 immunostainings and the changes by the treatment are shown in Fig. 2.

Relationship with clinical and pathological response to pre-CT. There was a positive correlation between clinical objective response and negativity of PgR status (p=0.0405, Chi-square test, Table II). Pre-treatment MIB-1 index and post-treatment MIB-1 index were associated with ER status significantly as shown in Table II (p=0.0018 and p=0.0021, respectively by Chi-square test). Neither pathological response nor M30 index showed a significant correlation with menopausal status, tumor size, nodal status and hormone receptor status. No significant correlation between clinical tumor response by pre-CT and M30 index, or MIB-1 index, was detected (data not shown). Any parameter, pre- and post-treatment index of M30 or MIB-1, or increase of M30 index during pre-CT, showed no significant association with clinical tumor response, but decrease of MIB-1 index during pre-CT showed significant association with clinical tumor response (data not shown). On the other hand, post-treatment M30 index increased significantly after pre-CT in histological response grade 2-3 cases (p=0.0188, t-test), whereas no significant increase was observed in histological response grade <2 patients (Fig. 3). Only one case that showed complete disappearance of tumor cells (pathological response grade 3) by pre-CT was included in this analysis.

Survival analysis. Survival analysis was conducted in a subgroup of 42 patients who underwent FAC therapy alone pre- and post-operatively, because this subgroup was a pure subset to assess the relationship of MIB-1/M30 status and therapeutic outcome of chemotherapy. No clinical CR was included in this analysis. Univariate analyses were conducted for post-treatment M30 index, post-treatment MIB-1 index and MIB-1/M30 ratio at every cut-off point by step-wise method, and it was found that >35, >140 and >5 showed the highest prognostic values for M30 index (p=0.0009), MIB-1 index (p=0.0014) and MIB-1/M30 ratio (p=0.0003) by log-rank test in disease-free survival (Table III). The tumors having <35 M30 index, having >140 MIB-1 index and >5 MIB-1/M30 ratio showed a